A Numerical Study of Flame Stabilization in Single Channel and Counter-flow Meso Scale Combustor

Muhammad Zahir Hassan[1,2] Fudhail Abdul Munir[3]
[1]Department of Industrial Design,
Eindhoven University of Technology, The Netherlands
[2]Faculty of Engineering Technology,
Universiti Teknikal Malaysia Melaka, Malaysia.
[3]Faculty of Mechanical Engineering,
Universiti Teknikal Malaysia Melaka, Malaysia

***Abstract*— The micro power generation system is one of the potential solutions that provides better energy requirement for small devices as compared to conventional batteries. In recent years, numerous works have been conducted to enhance the combustion stability of meso and micro-scale combustors. The utilization of heat recirculation mechanism is one of the approaches to enhance the flame stabilization limits in micro combustors. In this study, flame stabilization in a single channel and counter-flow cylindrical tube combustors with wire mesh was numerically studied. The wire mesh was located between the unburned and burned gas regions of the tubes. A three-dimensional numerical simulation was performed to establish vital parameters such as gas, wire mesh and outer wall temperature. For the validation of the numerical results, the flame blowout and extinction limits were first obtained and compared with experimental results. The utilization of the numerical model enables the improvement on design of the combustor where a counter-flow tube combustor with wire mesh is proposed. Both gaseous and liquid fuels can be used as the primary source for the tube combustor. In a micro power generation system, a combustor with liquid fuel source is preferred as it solves the mobility issue.**

***Index Term*— Micro power generation, micro-scale combustors, heat recirculation**

I. Introduction

The scarcity of energy resources and the high demand for better power sources as compared to conventional batteries have sparked research interest in micro power generation [1]. The new state of the art electronics devices requires greater energy capacity, shorter charging period and lightweight design, characteristics that batteries lack. Therefore, in recent years micro power generation systems have been seen as potential alternatives to batteries due to the higher energy densities of hydrocarbon fuels [2].

Stable flame in narrow channel combustors can be achieved by recirculating the heat produced from the combusted products to the incoming fuel mixture. In conventional combustor devices like the internal combustion engine, a portion of the burned product gasses is re-circulated and injected into the fuel-air mixture to reduce the amount of oxides of nitrogen (NO_X) [3]. On the other hand, in micro combustion applications, the purpose of heat recirculation is to minimize heat loss and to expand the flame stabilization limits. This heat recirculation concept was first proposed by Weinberg in 1971 [4]. The enthalpy from the hot burned gas is utilized to pre-heat the incoming fuel and air mixtures, which results in the enhancement of combustion reaction. This mechanism of flame stabilization is also known as excess enthalpy principle [5]. Generally, in an excess-enthalpy micro combustor, the flow of the reactants and combustion products occurs in the adjacent channel and in an opposite direction. This condition causes the unburned mixture being preheated by the high-temperature exhaust gas. Consequently, the total enthalpy is greatly increased [6].

There are two types of pre-heating methods [7]. The direct method is a condition where the heat is transferred through conduction and radiation from the burned gas to the unburned gas region. This direct method is normally applied to a single channel (SC) micro combustor. In such combustor, the heat from the burned gas region is axially transferred to the unburned gas region through the solid structure, resulting in better flame stabilization limits. On the other hand, the burned gas can be reversed to pre-heat the unburned reactants coming into the combustor inlet. This method is named as indirect pre-heating and mainly utilized in counter-current heat recirculation combustors.

Swiss-roll (SR) combustor is probably the most popular configuration for combustors with heat recirculation. This type of combustor employs indirect pre-heating mechanism. Despite the many advantages of Swiss-roll combustors, their complexity in terms of geometry and design parameters has made them difficult to be analytically and experimentally investigated. A counter-current heat recirculation combustor that also utilizes the concept of the indirect pre-heating method has been proposed. In a numerical study conducted by Ronney [8], a meso-scale counter current heat exchanger combustor was modeled and analyzed. The heat exchanger is modeled as a divider between the reactants and product stream. The combustion of the unburned gas occurs in a well-stirred reactor. The hot burned gas then flows through the exhaust outlet where the unburned gas on the other side is pre-heated by mean of conduction on both sides of the wall. This analysis is a simplified version of the complex phenomenon that occurs in a Swiss-roll combustor.

Flame can also be stabilized by inserting a bluff body in the combustion chamber of micro combustors [9]. A simple yet effective way of extending flame stabilization limits has been demonstrated by Wan et al. [9,10]. In their work, a bluff body is inserted into a planar micro channel combustor. The experimental result shows that blow off limits is greatly extended with the presence of the bluff body. The idea of using a flame holder in meso-scale cylindrical quartz tube combustors was first proposed by Mikami et al. [11]. In their experimental work, a stainless steel wire mesh is placed between the burned and unburned gas region. The experimental results show that flame can be stabilized for both gas and liquid fuel. In fact, it was also reported that the flame could even be stabilized in a tube combustor with an inner diameter below than the classical quenching distance. The wire mesh improves the heat transfer from the hot burned gas to the unburned gas region, resulting in better flame stabilization limits. Interestingly, no external heating is required to sustain the flame. The tube combustor with wire mesh can also be considered as the combustor with heat recirculation since the wire mesh effectively re-distributes the heat from the burned gas to the unburned gas region.

In this research, a numerical study of flame stabilization in a single channel and counter-flow tube combustor with wire mesh is presented. The tube combustor utilizes a stainless steel wire mesh that helps to stabilize the flame. A three-dimensional (3-D) is used as the numerical model. Munir and Mikami [12] stated that a two-dimensional model is not appropriate to represent geometry model of the tube combustor with wire mesh. The main reason of having a 3-D model is to include the effect of the thermal path from the wire mesh to the combustor outer wall. Two types of counter-flow tube combustors are then proposed to improve the flame stabilization. The later design of the counter-flow combustor is preferred since it can be used for both liquid and gaseous hydrocarbon fuels.

II. RESEARCH APPROACH

A. *Single channel tube combustor with wire mesh*

In the proposed single channel tube combustor, a stainless steel wire mesh is placed between the unburned and burned gas region as depicted in Fig. 1. The wire mesh plays an important role in distributing the heat from the hot burned gas region to the unburned gas region. The wire mesh plays an important role in distributing the heat from the burned gas region to the unburned gas region.

In order to simulate the flame stabilization in such narrow channel, numerical simulations using ANSYS Fluent were performed. Since the calculated range of Reynolds number is between 49 to 200, laminar finite-rate is utilized to solve the turbulence flow and combustion interaction. The gas density is calculated based on the ideal gas law while the specific heat of all the species is calculated using a piecewise-polynomial fit of temperature.

The mixing law and kinetic theory are employed to solve the specific heat and the thermal coefficient of the gas mixture. To reduce the computational time, overall single step propane-air combustion with five species is employed as the combustion chemistry [13,14]. Equation (1) presents the combustion chemistry.

$$C_3H_8 + 5O_2 \rightarrow 3CO_2 + 4H_2O \quad (1)$$

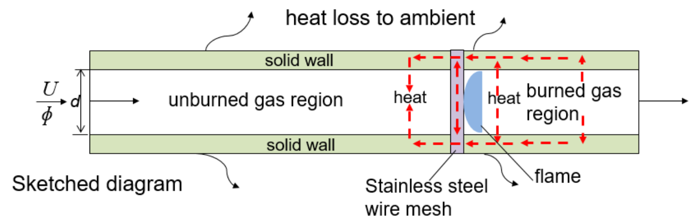

Fig. 1. Illustrated diagram of a single channel combustor with wire mesh

This single step reaction model is deemed sufficient since the focus of this study is to examine the flame stabilization phenomenon. A variable grid size is utilized where critical areas of computational domain especially in the burned gas region are given high grid concentration. The minimum grid size is 0.01 mm and the total number of elements is 43548 and employed for all cases. Higher number of elements provide no significant numerical advantage as the flame temperature is hardly changed. Fig. 2 summarizes the computational domain for a single channel tube combustor.

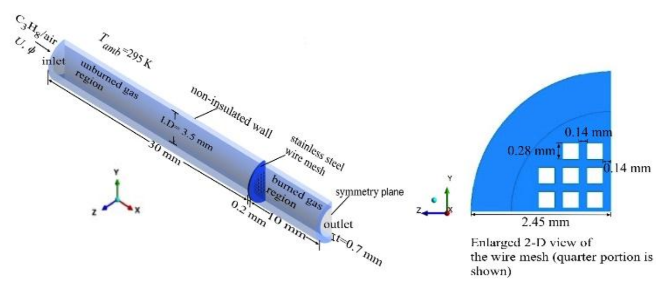

Fig. 2. Computational domain for the numerical simulations

Meanwhile, the governing equations utilized are the typical fluid motion combined with reacting flows [15]. The mass conservation equation (continuity) is given by;

$$\frac{\partial \rho}{\partial t} + \frac{\partial}{\partial x}(\rho u_x) + \frac{\partial}{\partial y}(\rho u_y) + \frac{\partial}{\partial z}(\rho u_z) = S_m \quad (2)$$

S_m is the source term. An example of this term is vaporization of liquid or any user-defined source. Nevertheless, in this numerical model the value of S_m is fixed to 0.

IJENS

For a steady state condition,

$$\frac{\partial \rho}{\partial t} = 0 \tag{3}$$

The momentum conservation equation in *x*-direction is

$$\frac{\partial \rho u_x}{\partial t} + \frac{\partial(\rho u_x u_x)}{\partial x} + \frac{\partial(\rho u_y u_x)}{\partial y} + \frac{\partial(\rho u_z u_x)}{\partial z} = -\frac{\partial p}{\partial x} - \frac{\partial}{\partial x}\left(\frac{2}{3}\mu(\nabla\cdot\vec{u}) + 2\mu\frac{\partial u_x}{\partial x}\right) + \frac{\partial}{\partial y}\left[\mu\left(\frac{\partial u_y}{\partial x} + \frac{\partial u_x}{\partial y}\right)\right] + \frac{\partial}{\partial z}\left[\mu\left(\frac{\partial u_x}{\partial z} + \frac{\partial u_z}{\partial x}\right)\right] + \rho f_x \tag{4}$$

while momentum equation in *y*-direction,

$$\frac{\partial(\rho u_x u_y)}{\partial x} + \frac{\partial(\rho u_y u_y)}{\partial y} + \frac{\partial(\rho u_z u_y)}{\partial z} = -\frac{\partial p}{\partial y} - \frac{\partial}{\partial x}\left[\mu\left(\frac{\partial u_y}{\partial x} + \frac{\partial u_x}{\partial y}\right)\right] + \frac{\partial}{\partial y}\left(\frac{2}{3}\mu(\nabla\cdot\vec{u}) + 2\mu\frac{\partial u_y}{\partial y}\right) + \frac{\partial}{\partial z}\left[\mu\left(\frac{\partial u_z}{\partial y} + \frac{\partial u_y}{\partial z}\right)\right] + \rho f_y \tag{5}$$

and momentum equation in *z*-direction is

$$\frac{\partial(\rho u_x u_z)}{\partial x} + \frac{\partial(\rho u_y u_z)}{\partial y} + \frac{\partial(\rho u_z u_z)}{\partial z} = -\frac{\partial p}{\partial z} - \frac{\partial}{\partial x}\left[\mu\left(\frac{\partial u_x}{\partial z} + \frac{\partial u_z}{\partial x}\right)\right] + \frac{\partial}{\partial y}\left[\mu\left(\frac{\partial u_z}{\partial y} + \frac{\partial u_y}{\partial z}\right)\right] + \frac{\partial}{\partial z}\left(\frac{2}{3}\mu(\nabla\cdot\vec{u}) + 2\mu\frac{\partial u_y}{\partial z}\right) + \rho f_z \tag{6}$$

where

$$\nabla\cdot\vec{u} = \frac{\partial u_x}{\partial x} + \frac{\partial u_y}{\partial y} + \frac{\partial u_z}{\partial z} \tag{7}$$

The energy transfers due to conduction, species diffusion and viscous dissipation are represented by the Eq. (8) and (9) respectively.

$$\nabla\cdot(\vec{u}(\rho E + p)) = \nabla\cdot\left(k\nabla\mathrm{T} - \sum_i h_i\vec{J}_i + (\bar{\bar{\tau}}\cdot\vec{u})\right) + S_h \tag{8}$$

$$\nabla\cdot(\vec{u}\rho h) = \nabla\cdot(k\nabla\mathrm{T}) + S_h \tag{9}$$

Here S_h is the heat of chemical reaction or any other volumetric heat sources added by the user. Eq. (8) and Eq. (9) has already included the pressure work and kinetic energy terms. However, the numerical model is assumed to be incompressible flows and neglects these types of works. For the species transport equation is defined as:

$$\nabla\cdot(\rho\vec{u}Y_i) = -\nabla\cdot\vec{J}_i + R_i + S_i \tag{10}$$

where R_i and S_i is the net rate of production of species *i* by chemical reaction and rate of creation by addition from the dispersed phase plus any user-defined sources. For the mass diffusion in laminar flows, Fluent employs the dilute approximation, which is also known as Fick's law to model the mass diffusion due to the concentration gradients. The equation for the mass diffusion is given as

$$\vec{J}_i = -\rho D_{i,m}\nabla Y_i - D_{T,i}\frac{\nabla T}{T} \tag{11}$$

The boundary treatment at the interface between the fluid and solid wall is assumed to be no-slip boundary type. The heat flux at this interface is calculated using Fourier's law. Heat transfer per unit area by means of convection and radiation at the outer surface of the combustor wall is given as

$$q_{loss} = h_{conv}(T_{wall} - T_{amb}) + \varepsilon\sigma(T_{wall}^4 - T_{amb}^4) \tag{12}$$

where, h_{conv} is the convective heat transfer coefficient, T_{wall} is the wall temperature of the combustor and T_{amb} is defined as the ambient temperature. The value of T_{amb} is initialized to 295 K. The value of h_{conv} is fixed to be at constant 5 W/m^2K. The external emissivity *(ε)* for the outer wall is selected based on the material type of the combustor while the value of *ε* for the wire mesh is set 0.70. The value of Stefan-Boltzmann constant *(σ)* used is 5.67 x 10^{-8} W/m^2K^4.

A thermal insulation (zero heat flux boundary) is applied at both left and right wall edge of the combustor. For the outlet boundary condition, a fixed pressure inlet is applied. A symmetrical boundary condition is established at the origin of z-plane so that the calculation can be performed only in half of the domain. The material thermal properties and the gas transport data are obtained from the Fluent internal database [15] and Kutz [16].

IJENS

Initially, the momentum and continuity equation is solved. Then, the energy and species equations are solved by applying a sufficiently high temperature of 1600 K to the patching zone, which is defined 1 mm from the outlet. Once ignited, the flame propagates to the upstream and eventually stabilizes near the wire mesh. With a fixed equivalence ratio (ϕ), both blowout and extinction limits are obtained by gradually changing the inlet flow velocity.

B. *Counter-flow tube combustor with wire mesh*

The flame stabilization limits of the single channel tube combustor can be further improved. One of the ways to enhance the flame stabilization is by inserting the combustor into an outer tube. Fig. 3 shows the diagram of the combustor. The outer tube is assumed to be made of the quartz tube. The exterior heat losses through the outer wall are in the form of convection and radiation. The value of the convective heat transfers coefficient (*h*) is 5 W/m^2K while the emissivity is fixed to 0.9. Quartz is assumed to be the material for both the combustor and outer tube. The thickness of the outer tube is set to 1 mm by activating the shell conduction in Fluent. The material for both the combustor and outer tube is assumed to be made of quartz, which means that the *k* value is fixed to 1.6 W/m/K.

A cold flow simulation condition is first performed in which only the continuity and momentum equations are solved. All results are presented in the next sub-section.

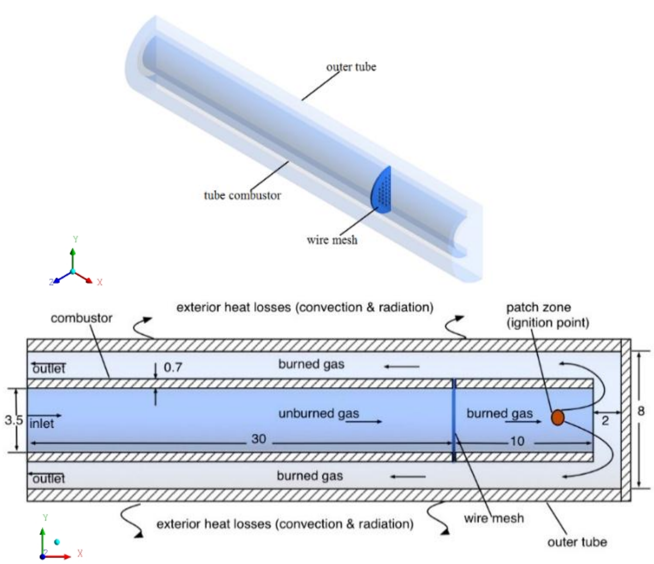

Dimensions are in mm

Fig. 3. Computational domain for counter-flow tube combustor

III. RESULTS AND DISCUSSION

A. *Flame stabilization in a single channel tube combustor*

Flame stabilization limits for the single channel tube combustor with wire mesh are numerically examined. Blowout and extinction limits are the examples of flame stabilization indicators in meso and micro-scale tube combustors. Both limits for this type of combustor are presented in Fig. 4. In order to ensure that the numerical model is credible, experiments were also conducted to determine the stability limits. The similar experimental configuration as proposed by Mikami et al. [11] is utilized.

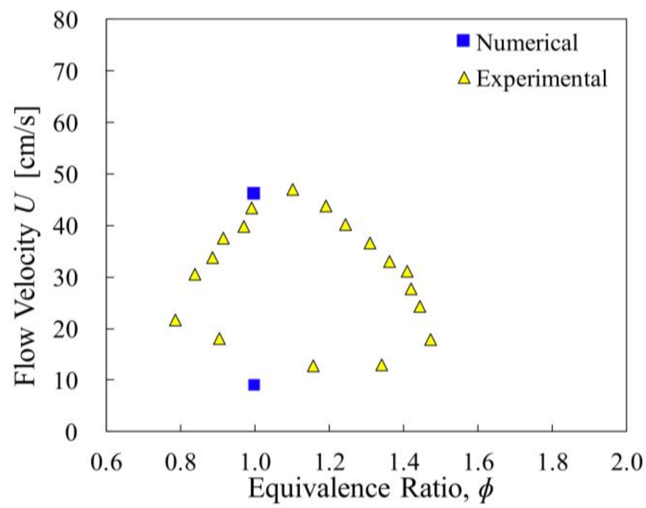

Fig. 4. The numerically determined blowout and extinction limits

The results obtained from the experiment are plotted on the same graph. The predicted value of the blowout limit at ϕ=1.0 is U=46 cm/s, which is higher than the experimental result. On the contrary, a reverse pattern is observed for the extinction limit. These notable differences are mainly due to the reduced one-step propane reaction that has over-predicted the flame temperature.

B. *Flame stabilization in a counter-flow tube combustor*

A cold flow simulation condition is first performed in which only the continuity and momentum equations are solved. The results of local velocity magnitude and streamline pattern are depicted in Fig. 5 while the results with energy and specified equations solved are shown in Fig. 6.

As seen in Fig. 6, the wire mesh temperature is significantly high. This elevation of temperature is mainly because there is no straight thermal path from the wire mesh to the ambient air. As for the gas, combustor wall, and outer tube temperature contours, the results are generally within the expectation. Since the outer tube is assumed to be made of quartz glass, it can be seen that much of the heat is only concentrated within a small area. In other words, there is high thermal stress occurs on the combustor and outer tube wall.

It is important to note that in order to include the outer tube in the numerical model, a total of 188043 nodes need to be utilized. This high number of nodes require longer computational time especially in determining the blowout limits.

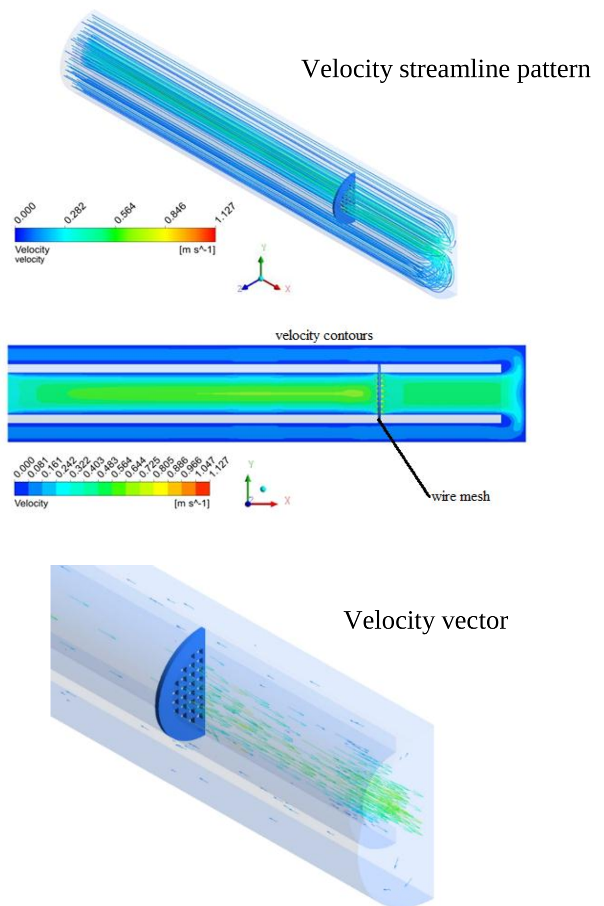

Fig. 5. Cold flow simulation local velocity results with U=35 cm/s

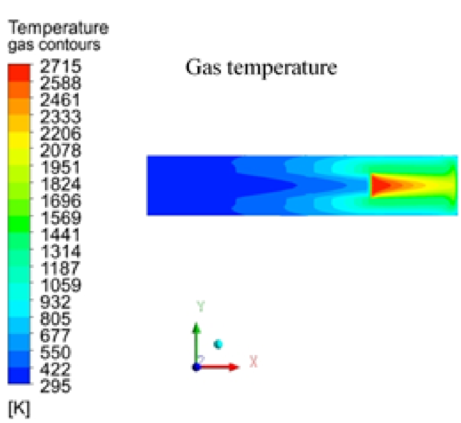

(a)

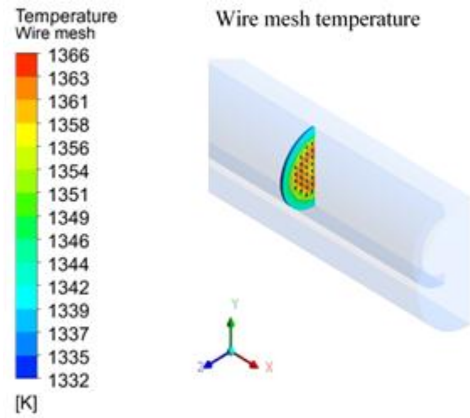

(b)

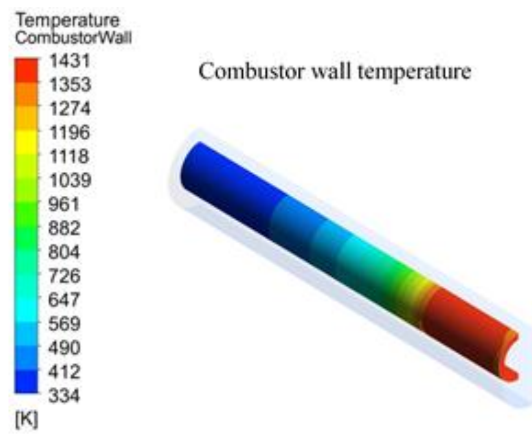

(c)

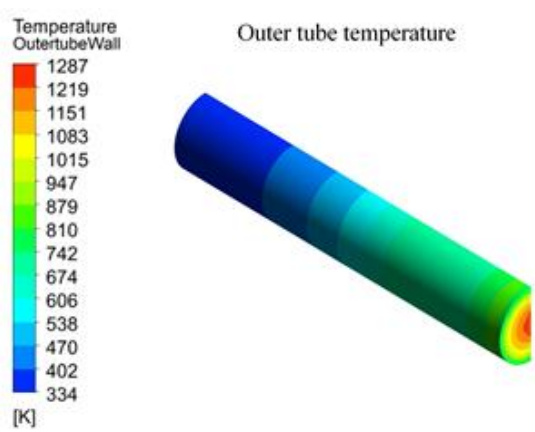

(d)

Fig. 6. Temperature contours for U=35 cm/s and ϕ=1.0 (a) Gas temperature (b) Wire mesh temperature (c) Combustor wall temperature (d) Outer tube temperature

IJENS

IV. DESIGN IMPROVEMENT OF COUNTER FLOW TUBE COMBUSTOR

A. *Reduction of tube combustor outer diameter*

The findings obtained from the numerical and simulation works are utilized as the guideline to properly design a meso-scale tube combustor with heat recirculation mechanism. It is desirable to have a combustor with high blowout limits as high power output can be achieved with a high flow velocity.

To improve the practicality of the combustor, the inner diameter of the outer tube is suggested to be reduced to 6 mm. The effect of the diameter reduction on the combustion characteristics is then numerically examined. The computational domain and results obtained from the simulations are depicted in Fig. 7 and 8. The exterior heat losses through the outer wall are assumed to be in the form of convection and radiation. The value of the convective heat transfers coefficient (h) is fixed to 5 W/m^{2}K while the emissivity is set to 0.9. Quartz is assumed to be the material for both the combustor and outer tube.

As seen in Fig. 8, there is a small drop of flame temperature as compared to the outer tube with 8 mm of inner diameter. It is expected that the flame stabilization limits should not be significantly affected. The blowout limit with this new condition is 65 cm/s for equivalence ratio (ϕ) equal to 1.0. The limitation of the below design combustor is that only gaseous fuels can be utilized as the primary source of fuel. This limitation defeats the main purpose of having micro power generation system, which is portability.

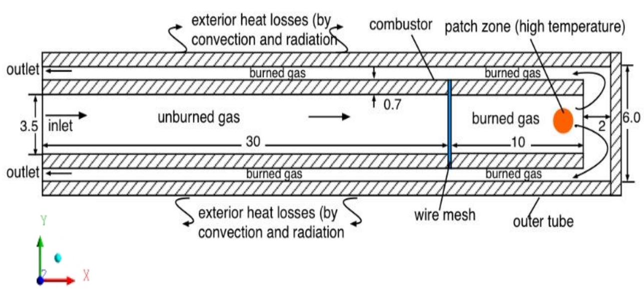

Fig. 7. Computational domains for outer tube with inner diameter of 6 mm (*dimension in mm*)

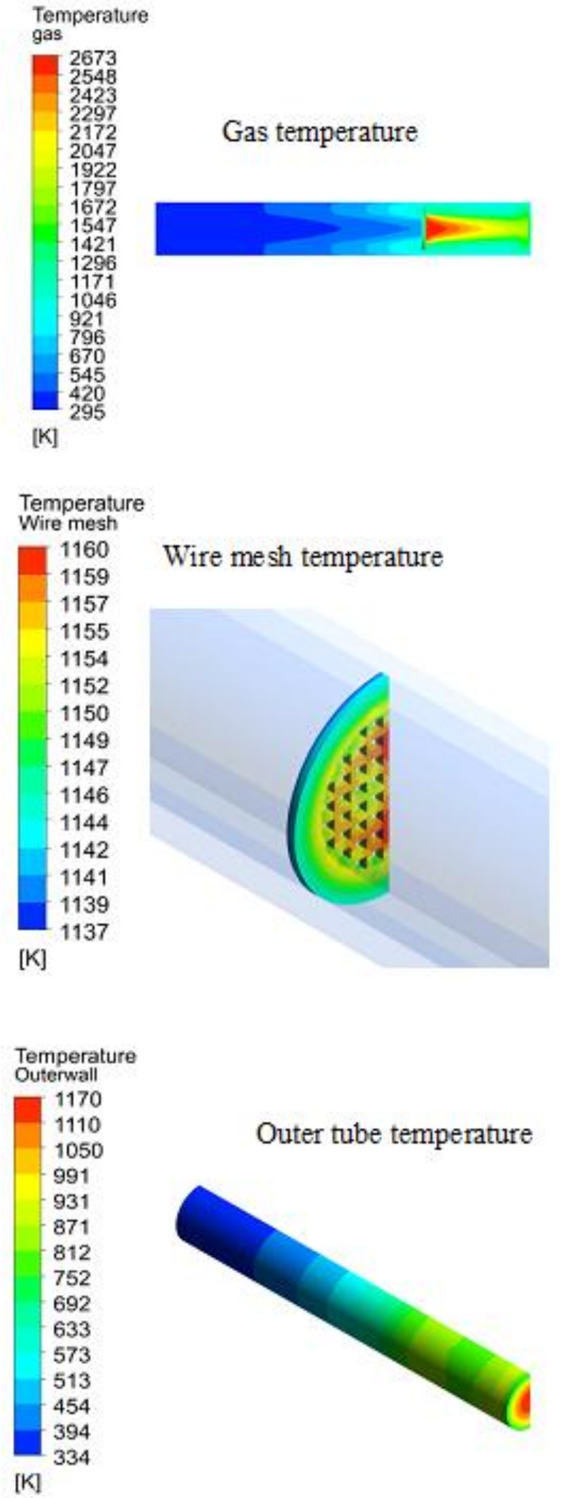

Fig. 8. Simulation results for *U*=35 cm/s and ϕ=1.0 for outer tube with inner diameter of 6 mm

B. Tube combustor for gaseous and liquid fuel

It is desirable that an improved design of combustor can also be used for liquid fuels. The use of liquid fuel eliminates the problem of tube combustor mobility. Droplets of liquid fuel can be generated with the utilization of electrospray technique as proposed by Yuliata et al. [17]. In order to apply the electrospray method on the combustor, a minimal modification needs to be performed. The direction of inlet flow of combustor needs to be reversed. The gas should be supplied through the small gap between the combustor and the outer tube.

The sketched diagram of the proposed combustor is presented in Fig. 9(a). The effect of changing the flow of gas is then numerically examined, where the computational domain is shown in Fig. 9(b). Both of the combustor and outer tube is assumed to be made of quartz. Results of the numerical simulations are presented in Fig. 10.

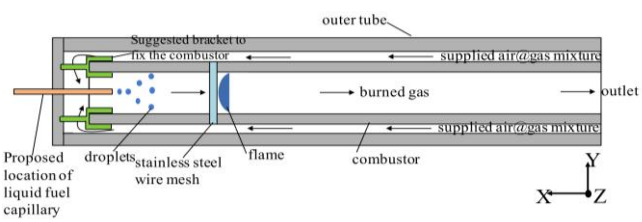

(a) Illustration of the proposed combustor with gas and liquid fuel

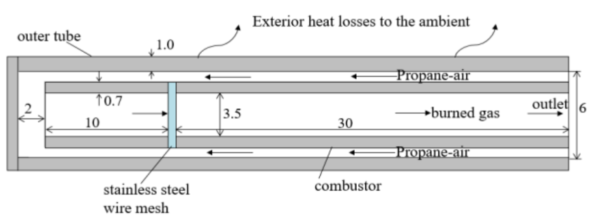

(b) Computational domain for propane-air simulation (*dimension in mm*)

Fig. 9 Proposed tube combustor for the use of liquid and gaseous fuel

Since the average cross-sectional area of the inlet is the same as the average cross-sectional area of the inlet in combustor shown in sub-section of IV-A, direct comparison of the flow velocity can be made. As shown in Fig. 10, the flame temperature is slightly increased as compared to results in Fig. 8, but the increment can be considered as insignificant. The increase of the flame temperature causes a modest elevation of the outer wall and wire mesh temperature. However, it can be seen from the figure that there is a notable upward change on the unburned gas temperature.

This finding is further corroborated from the graph of gas temperature along the centerline of the combustor as depicted in Fig. 11. The calculated mass-weighted average of the unburned gas temperature for the proposed tube combustor for the liquid fuel is given as 711 K. On another hand, the average temperature for the case in sub-section of IV-A is calculated as 641 K. Thus, it is predicted that flame stabilization can be enhanced with the change of the inlet flow direction.

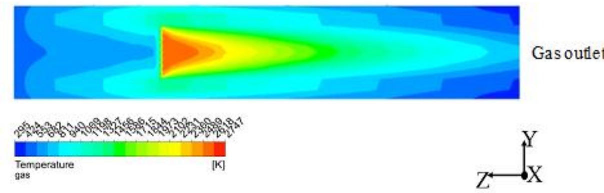

(a) Gas temperature

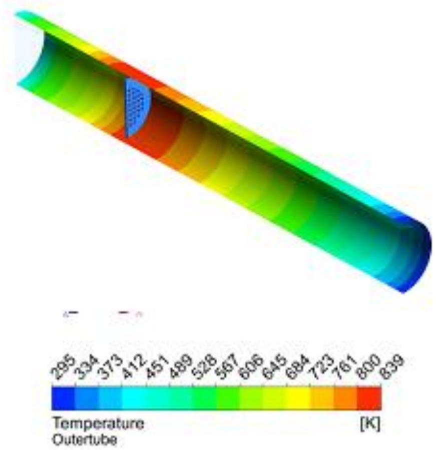

(b) Outer tube wall temperature

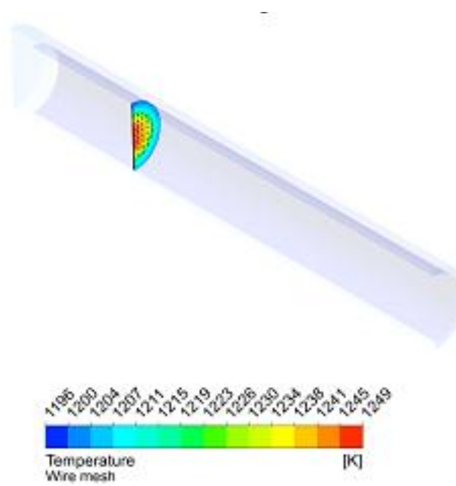

(c) Wire mesh temperature

Fig. 10. Simulation results for proposed counter-flow tube combustor with wire mesh for U=35 cm/s and ϕ=1.0

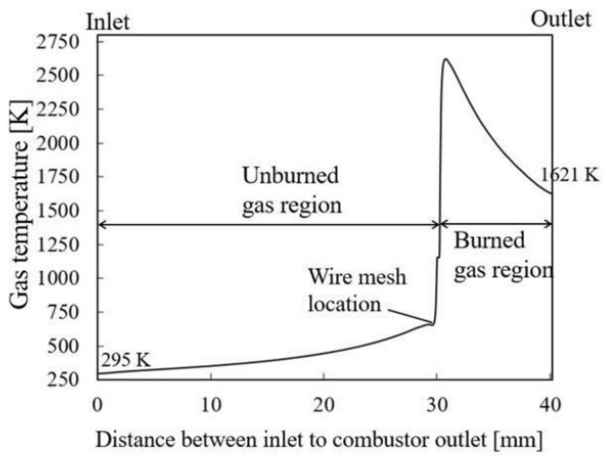

(a) Counter-flow tube combustor for gaseous fuel only (section IV-A)

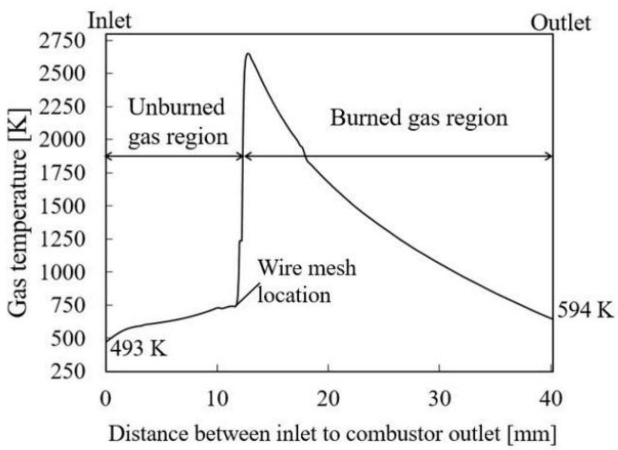

(b) Proposed combustor for liquid and gaseous fuels

Fig. 11. Gas temperature along the centerline of combustor for U=35 cm/s and ϕ=1.0

V. CONCLUSION

A numerical study of flame stabilization in single channel and counter-flow tube combustors with wire mesh has been demonstrated. A three-dimensional numerical model was utilized to investigate vital factors that might affect the flame stabilization limits. For validation purposes, the obtained flame blowout and extinction limits are compared with experimental results. Although there is a significant discrepancy between the numerical and experimental results, the difference is understandable since a single step combustor chemistry is utilized. The numerical model is then used to establish essential parameters such as gas,wire mesh, and wall temperatures. A counter-flow tube combustor with wire mesh is also proposed. Two types of counter-flow combustors are presented. In order to use a liquid fuel such as heptane, the inlet of the counter-flow combustor is reversed. It is important to note that the exhaust gas does not mix up with the unburned reactants. This characteristic makes the proposed combustor different than conventional Exhaust Gas Recirculation (EGR) system.

ACKNOWLEDGMENT

The authors would like to thank Ministry of Higher Education Malaysia (MoHE) and Universiti Teknikal Malaysia Melaka (UTeM) for the research funding.

REFERENCES

[1] K. Maruta, “Micro and mesoscale combustion,” Proceedings of the Combustion Institute, Vol. 33, pp. 125-150, 2011.

[2] Y. Ju and K. Maruta, “Microscale combustion: Technology development and fundamental research,” Progress in Energy and Combustion Science, Vol. 37, pp. 669-715, 2011.

[3] S.R. Turns, An Introduction To Combustion Concepts and Applications, Singapore: Mc Graw Hill, 2000.

[4] V.V. Zamashchikov, “Experimental Investigation of gas combustion regimes in narrow tubes,” Combustion and Flame, Vol. 108, pp. 357-359, 1997.

[5] L. Sitzki, K. Borer, E. Schuster, P.D. Ronney and S. Wussow, “Combustion in Microscale Heat-Recirculating Burners,” The Third Asia-Pacific Conference on Combustion, June 24-27, 2001.

[6] Z. Bei-Jing and W. Jian-Hua, “Experimental study on premixed CH4/air mixture combustion in micro Swiss-roll combustors,” Combustion and Flame, Vol. 157, pp. 2222-2229.

[7] S. Raimondeau, D. Norton, D.G. Vlachos and R.I. Masel, “Modeling of high temperature microburners,” Proceedings of the Combustion Institute, Vol. 29, pp. 901-907, 2002.

[8] P.D. Ronney, “Analysis of non-adiabatic heat-recirculating combustors,” Combustion and Flame, Vol. 135, pp. 421-439, 2003.

[9] J. Wan, A. Fan, K. Maruta, H. Yao and W. Liu, “Experimental and numerical investigation on combustion characteristics of premixed hydrogen/air flame in a micro-combustor with a bluff body,” International Journal of Hydrogen Energy, Vol. 37, pp. 19190-19197, 2012.

[10] A. Fan, J. Wan, Y. Liu, B. Pi, H. Yao and W. Liu, “Effect of bluff body shape on the blow-off limit of hydrogen/air flame in a planar micro-combustor,” Applied Thermal Engineering, Vol. 62, pp. 13-19, 2014.

[11] M. Mikami, Y. Maeda, K. Matsui, T. Seo and L. Yuliati, “Combustion of gaseous and liquid fuels in meso-scale tubes with wire mesh,” Proceedings of the Combustion Institute, Vol. 34, pp. 3387-3394, 2013.

[12] F.A. Munir and M. Mikami, “A numerical study of propane-air combustion in meso-scale tube combustors with concentric rings,” Journal of Thermal Science and Technology, Vol. 10, pp. 1-12, 2015.

[13] C.K. Westbrook and F.L. Dryer, “Simplified Reaction Mechanism for the Oxidation of Hydrocarbon Fuels in Flames,” Combustion Science and Technology, Vol. 27, pp. 31-43, 1981.

[14] D.G. Norton, D.G. Vlachos, “A CFD study of propane/air microflame stability,” Combustion and Flame, Vol. 138, pp. 97-107, 2004.

[15] ANSYS 15 Fluent Tutorial Guide, Ansys Inc., 2013.

[16] M. Kutz, Mechanical Engineers Handbook, USA: John Wiley & Sons, 1998.

[17] L. Yuliati, T. Seo and M. Mikami, “Liquid-fuel combustion in a narrow tube using an electrospray technique,” Combustion and Flame, Vol. 159 (1), pp. 462-464, 2012.

IJENS